Notch signaling in stomach epithelial stem cell homeostasis

Tae-Hee Kim[1,2,3] and Ramesh A. Shivdasani[1,2,3]

[1]Department of Medical Oncology, Dana-Farber Cancer Institute, Boston, MA 02115
[2]Department of Medicine, Brigham and Women's Hospital, Boston, MA 02115
[3]Department of Medicine, Harvard Medical School, Boston, MA 02115

The mammalian adult gastric epithelium self-renews continually through the activity of stem cells located in the isthmus of individual gland units. Mechanisms facilitating stomach stem and progenitor cell homeostasis are unknown. Here, we show that Notch signaling occurs in the mouse stomach epithelium during development and becomes restricted mainly to the isthmus in adult glands, akin to its known localization in the proliferative compartment of intestinal villi. Using genetic and chemical inhibition, we demonstrate that Notch signaling is required to maintain the gastric stem cell compartment. Activation of Notch signaling in lineage-committed stomach epithelial cells is sufficient to induce dedifferentiation into stem and/or multipotential progenitors that populate the mucosa with all major cell types. Prolonged Notch activation within dedifferentiated parietal cells eventually enhances cell proliferation and induces adenomas that show focal Wnt signaling. In contrast, Notch activation within native antral stomach stem cells does not affect cell proliferation. These results establish a role for Notch activity in the foregut and highlight the importance of cellular context in gastric tumorigenesis.

CORRESPONDENCE
Ramesh A. Shivdasani:
ramesh_shivdasani@dfci.harvard.edu

Abbreviations used: DBZ, dibenzazepine; EdU, 5-ethynyl-2'-deoxyuridine; EE, enteroendocrine; NICD, Notch1 intracellular domain.

Self-renewing epithelia in the stomach and intestine share common features, including stem cell activity. Transit-amplifying progeny of these stem cells replicate briskly and differentiate in the small bowel into enterocytes and secretory cells, and in the glandular stomach into four principal daughter lineages: foveolar (pit), oxyntic (parietal), zymogenic (chief), and enteroendocrine (EE) cells. The stomach body or corpus is organized in monoclonal gland units that contain a luminal surface pit (foveolus), leading to a narrow isthmus, a short neck, and a wide base (see also Fig. 2 A). [^{3}H]thymidine autoradiography and ultrastructural features place gastric stem cells in the isthmus (Hattori and Fujita, 1976; Lee et al., 1982). From this location, pit cells migrate toward the lumen, whereas zymogenic, EE and most parietal cells migrate toward the base (Karam and Leblond, 1993). In the distal stomach, or antral-pyloric segment, glands are short and carry rare chief or parietal cells but abundant mucous and EE cells (Lee and Leblond, 1985). Stem cells in this part of the stomach lie close to the gland base, and like their counterparts in the intestine, the crypt base columnar cells (Barker et al., 2007), they express the cell surface marker Lgr5 (Barker et al., 2010). Wnt–β-catenin signaling, in particular, is essential for proliferation of intestinal crypt cells (van der Flier and Clevers, 2009), but its functional requirement in most gastric stem cells is unclear.

The intestinal epithelium also responds to the Notch signaling pathway, inactivation of which arrests cell replication and induces secretory cell metaplasia (van Es et al., 2005). Unregulated Notch signaling in the fetal intestine enhanced cell proliferation and inhibited goblet and EE cell differentiation in one study (Fre et al., 2005) and caused reversible progenitor loss and villus dysmorphogenesis in another (Stanger et al., 2005). Furthermore, Notch and Wnt signaling seem to cooperate in intestinal tumorigenesis (Fre et al., 2009; Rodilla et al., 2009). Targeted disruption of *Hes1*, a presumptive target of Notch signaling (Iso et al., 2003), increases the number of EE cells in the stomach and intestine (Jensen et al., 2000). Recent evidence suggests that Notch regulates progenitor proliferation and secretory cell differentiation through a single

Supplemental material can be found at:
http://doi.org/10.1084/jem.20101737

The Rockefeller University Press $30.00
J. Exp. Med. Vol. 208 No. 4 677-688
www.jem.org/cgi/doi/10.1084/jem.20101737

intestine-restricted basic helix–loop–helix transcription factor, Math1 (Kazanjian et al., 2010; van Es et al., 2010; Kim and Shivdasani, 2011). Because Math1 is not expressed in the stomach (Yang et al., 2001), Hes1 functions in stomach EE cell differentiation must occur through a Notch- or Math1-independent pathway (Jensen et al., 2000). It is also unknown if the Notch pathway affects gastric corpus progenitors, which are not strictly Wnt dependent, or promotes gastric tumorigenesis as it does in cooperation with Wnt in the intestine (Fre et al., 2009; Rodilla et al., 2009).

Here we report that Notch signaling begins early in stomach epithelial development and is largely confined to the proliferative zone in the isthmus of adult glands. Inhibition of Notch function impairs proliferation and has a modest effect on cell lineage allocation. Remarkably, Notch activation in lineage-committed stomach epithelial cells converts them into progenitors that produce all daughter cell types. Over time, proliferation of these dedifferentiated progenitors accelerates, leading to formation of dysplastic adenomas that show focal activation of Wnt signaling. In contrast, Notch activation by the same means in Lgr5$^+$ antral-pyloric stem cells preserves the normal pattern of cell proliferation. Collectively, these results reveal a requirement for Notch signaling in epithelial cell proliferation throughout the digestive tract and new, context-dependent roles for Notch in gastric stem cell homeostasis and tumorigenesis.

RESULTS

Inhibition of Notch signaling in embryonic mouse stomach exposes a competitive disadvantage

We examined expression of all Notch receptors, Notch1–4, ligands (Jagged1 and 2 and Delta-like 1, 3, and 4), and its best characterized target gene, *Hes1* (Ohtsuka et al., 1999), during mouse gut development, using RNA in situ hybridization at embryonic days (E) 12, 14, 15, and 17. Multiple ligands and receptors are expressed in fetal gastric epithelium, especially the Notch1 receptor and Jagged2 and Delta3 ligands (Fig. 1 A; Fig. S1; and not depicted); subepithelial signals were proportionately weaker. Consistent with expression of the signaling components, we readily detected Hes1 mRNA and protein in embryonic stomach epithelium (Fig. 1, A and B).

To examine the requirement for Notch signaling in stomach development, we first tested a conditional loss-of-function mutation in mice. As multiple ligands and receptors could be functionally redundant, we focused on the obligate Notch effector RBP-Jκ, also known as CSL (Kopan and Ilagan, 2009). Cre recombinase-dependent disruption of *RBP-Jκ* is an established tool to interrogate Notch function (Han et al., 2002). To express Cre in fetal stomach, we used *Osr1-Cre* transgenic mice, which transiently express Cre in the gut endoderm around E11 (Grieshammer et al., 2008). Crosses between *Osr1-Cre* and *Rosa26^{YFP}* reporter mice (Srinivas et al., 2001) confirmed mosaic expression throughout the E15 digestive tract, and subsequent crosses yielded *Osr1-Cre*;*RBP-Jκ$^{Fl/Fl}$*;*Rosa26^{YFP}* progeny in Mendelian ratios. *RBP-Jκ$^{Fl/Fl}$* mutant and *RBP-Jκ$^{+/Fl}$* controls showed a mean of 67 and 72% YFP$^+$ gut endodermal cells at E15, respectively (Fig. 1 C), reflecting mosaic Cre-mediated recombination in their precursors. Consistent with the growth stimulatory effect attributed to Notch in intestinal progenitors (van Es et al., 2005) and known effects of crypt competition, YFP$^+$ villi declined by 70% in 6-wk-old *Osr1-Cre*;*RBP-Jκ$^{Fl/Fl}$*;*Rosa26^{YFP}* intestines compared with *Osr1-Cre*;*RBP-Jκ$^{+/Fl}$*;*Rosa26^{YFP}* controls (Fig. 1 C). Similarly, YFP$^+$ gastric gland units were reduced by 47% compared with control animals (Fig. 1 C). Thus, *RBP-Jκ*–null intestinal and stomach epithelia both face a significant competitive disadvantage, allowing rapid dominance by clonal units that are proficient in Notch signaling.

In adult mouse intestine, conditional RBP-Jκ inactivation or Notch inhibition by γ-secretase inhibitors arrests crypt cell proliferation and induces goblet cell metaplasia (van Es et al., 2005). As neither of these defects was evident in YFP$^+$ villi of adult *Osr1-Cre*;*RBP-Jκ$^{Fl/Fl}$*;*Rosa26^{YFP}* intestines (Fig. 1 D), we considered the possibility that transient Cre expression in *Osr1-Cre* mice caused inefficient recombination at the *RBP-Jκ* locus, allowing residual Notch activity in both the YFP$^-$ (as a result of no recombination [mosaicism]) and YFP$^+$ (as a result of recombination at the ROSA26YFP locus and monoallelic recombination at one *RBP-Jκ^{Fl}* locus) daughter cells. To test this possibility, we isolated YFP$^+$ cells using flow cytometry and genotyped *RBP-Jκ* alleles using PCR (Laky and Fowlkes, 2007). Indeed, adult YFP$^+$ cells showed evidence for both deleted and nondeleted floxed sequences, confirming incomplete recombination (Fig. 1 E). Nevertheless, significantly reduced representation of YFP$^+$ cells in the adult *Osr1-Cre*;*RBP-Jκ$^{Fl/Fl}$*;*Rosa26^{YFP}* gut (Fig. 1 C) provides genetic evidence of a requirement for Notch signaling in maintenance of self-renewing stem cells.

Notch pathway inhibition in adult stomach arrests epithelial proliferation

Hes1 expression in the adult mouse intestine is restricted to proliferating crypt progenitors (Schröder and Gossler, 2002; van Es et al., 2005). Likewise, in adult stomach, Hes1 antibody (Ab) stained cells in the isthmus of corpus (Fig. 2 B) and antral (Fig. 2 C) glands, and most but not all Hes1$^+$ cells co-express the proliferation marker Ki67. These results suggest that Notch also signals in proliferating adult stomach cells. To inactivate Notch signaling in wild-type adult mice, we used the known Notch antagonist dibenzazepine (DBZ; Milano et al., 2004; Riccio et al., 2008). As others have reported (van Es et al., 2005), administration of 20 μmol/kg for 5 d arrested cell replication and induced severe goblet cell metaplasia in the intestine (Fig. S2, A and B). DBZ treatment also abolished Hes1 immunostaining in intestinal crypts and the isthmus of gastric glands (Fig. S2 C), indicating pathway-specific effects. Although stomach epithelial proliferation was only mildly reduced at the end of the 5-d treatment, proliferation in corpus and antral glands was virtually abolished 2 d later, leaving few Ki67$^+$ cells in some isthmi and no Ki67$^+$ cells in most glands (Fig. 2, D and E). Notch inhibition also resulted in increased numbers of Alcian blue–avid mucous cells at the

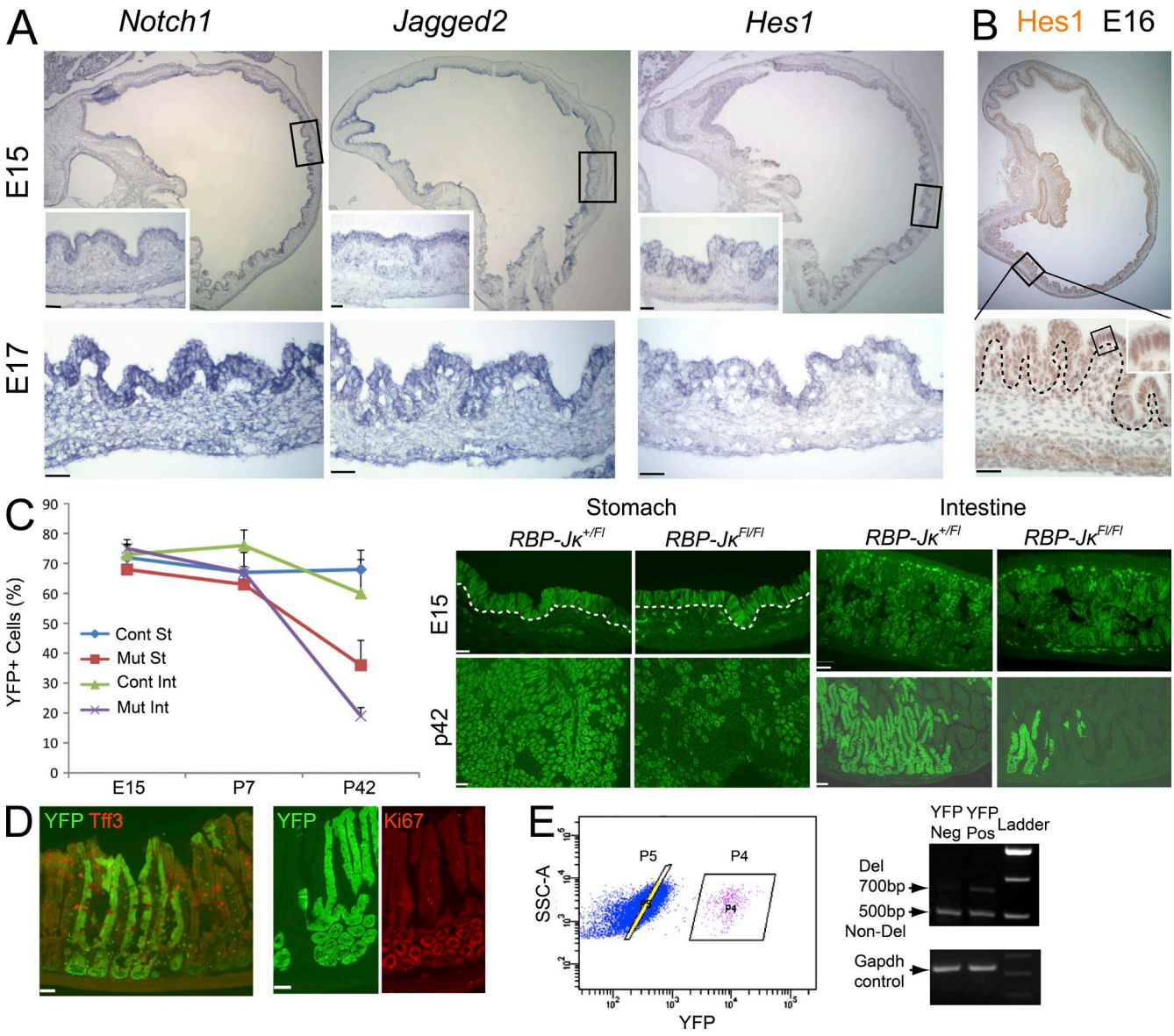

Figure 1. Expression of Notch signal components and their role in development of gastric gland units. (A) In situ hybridization for *Notch1*, *Jagged2*, and the Notch target gene *Hes1* in E15 and E17 mouse stomach epithelium. Boxed areas are shown at higher magnification in the insets. Additional data appear in Fig. S1. (B) Hes1 immunostaining of E16 mouse stomach. (C) Clonal YFP$^+$ gastric gland units and intestinal villi in *Osr1-Cre*;*RBP-Jκ$^{Fl/Fl}$*;*Rosa26^{YFP}* (MUT) mice compared with *Osr1-Cre*;*RBP-Jκ$^{+/Fl}$*;*Rosa26^{YFP}* (CONT) controls. Counts at E15 represent endodermal cells; at P7 and P42, the counts represent villi (intestine, Int) or glands (stomach, St). Representative examples of stomach and intestine YFP staining are shown from E15 mouse embryos and 42-d-old adults. Dotted lines demarcate the mesenchyme-epithelium boundary; trace mesenchymal signal is a blood vessel artifact. (D) Staining of adult (6 wk) *Osr1-Cre*;*RBP-Jκ$^{Fl/Fl}$*;*Rosa26^{YFP}* intestine with trefoil factor 3 (TFF3, left, co-stain) and Ki67 (right two panels, serial sections) Ab. (E) Flow sorting of YFP$^-$ (gate P5) and YFP$^+$ (gate P4) cells, followed by PCR genotyping for recombination at the *RBP-Jκ* locus (right). Preservation of LoxP-flanked *RBP-Jκ* sequences in YFP$^+$ cells indicates inefficient, likely monoallelic Cre-mediated deletion. The deleted and nondeleted *RBP-Jκ* alleles give 700- and 500-bp PCR products, respectively (Laky and Fowlkes, 2007). GAPDH provides a positive control. Bars, 50 µm. Quantitation in C was made using three embryos or mice per group; all other experiments were repeated twice with similar results.

base of antral glands (Fig. 2 F) and a small increase in corpus chromogranin A$^+$ EE cells (Fig. S2 D). 5 d of DBZ exposure led to death by day 8, precluding assessment of delayed effects. These results demonstrate a role for Notch signaling in gastric epithelial proliferation, parallel to that in Wnt-dependent intestinal crypts.

Activation of Notch signaling in parietal cells confers stem cell properties

The restriction of Notch pathway activity to progenitor cells (Fig. 2, B and C) prompted us to test the consequences of ectopic Notch signaling in differentiated cells, using transgenic mice that express Cre recombinase under control of

the parietal cell–specific H^+/K^+-*ATPase* β-*subunit* (*Atp4b*) promoter (Syder et al., 2004). To delineate the domain of Cre expression, we crossed *Atp4b-Cre* and *Rosa26*^{YFP} mice. YFP signal appeared in all *Atp4b*-expressing cells (Fig. 3 A and Fig. S3 A), confirming the reported lineage-restricted pattern (Syder et al., 2004). A few basally located YFP$^+$ cells failed to stain with Atp4b Ab, but expressed the chief cell-specific product, gastric intrinsic factor (Gif, Fig. 3 C); however, most Gif$^+$ cells did not express YFP and, as expected, Atp4b and Gif staining never overlapped (Fig. S3 B). These results suggest that Cre might express in bipotential progenitors of parietal and chief cells. To examine this possibility, we treated mice with the S-phase label 5-ethynyl-2'-deoxyuridine (EdU). In the isthmus of rare glands, we observed YFP-positive cells that lacked Atp4b but had incorporated EdU, indicating recent cell replication (Fig. 3, A and B, arrows). As expected, the proliferation marker EdU and the Atp4b marker of terminal parietal cytodifferentiation did not overlap

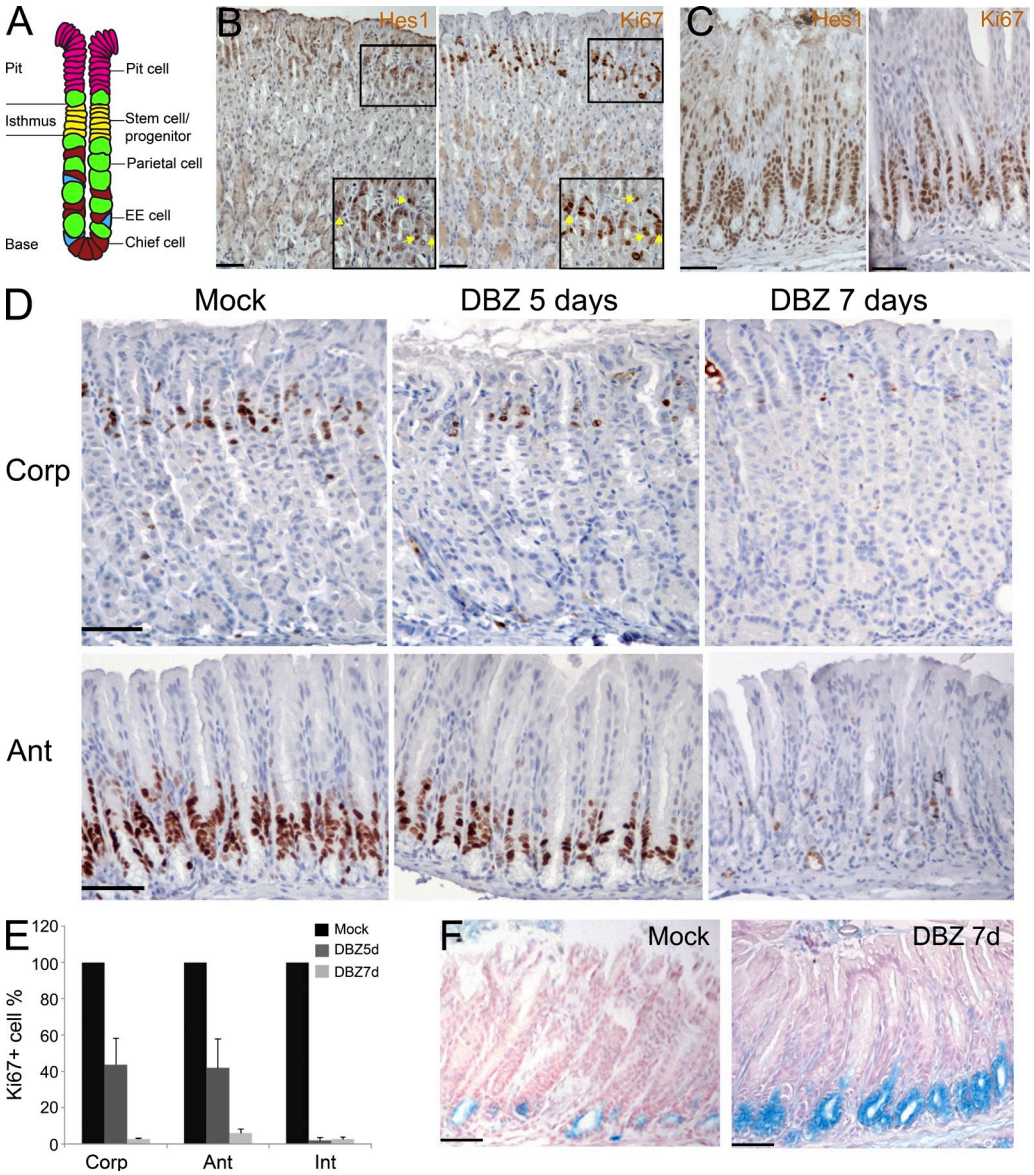

Figure 2. Role of Notch in proliferation of adult gastric epithelial progenitors. (A) Diagram of a glandular unit in adult gastric corpus. Stem cells in the isthmus give rise to four major progeny: pit, chief, parietal, and EE cells. (B) Hes1 and Ki67 expression in the isthmus of gland units in the adult gastric corpus. Sequential tissue sections reveal coexpression of Hes1 and proliferation marker Ki67 (arrows). Hes1 luminal surface staining is nonspecific. Boxed areas are shown at higher magnification in the insets. (C) Coexpression of Hes1 and Ki67 in the isthmus of antral glands, where both markers are expressed in cells closer to the base than in the corpus. (D) Adult gastric epithelial Ki67 expression 5 and 7 d after administration of 20 µmol/kg DBZ in 0.5% METHOCEL E4M or 0.5% METHOCEL E4M only (Mock). (E) Quantitation of proliferating cells in stomach glands after DBZ exposure. Bars represent mean ± SD. (F) Alcian blue stain reveals antral mucous cells. Bars, 50 µm. Analysis in E was done using three mice per group. Experiments in F used three mice, with staining done in duplicate; all other experiments were repeated twice, with similar results. Corp, corpus; Ant, antrum; Int, intestine.

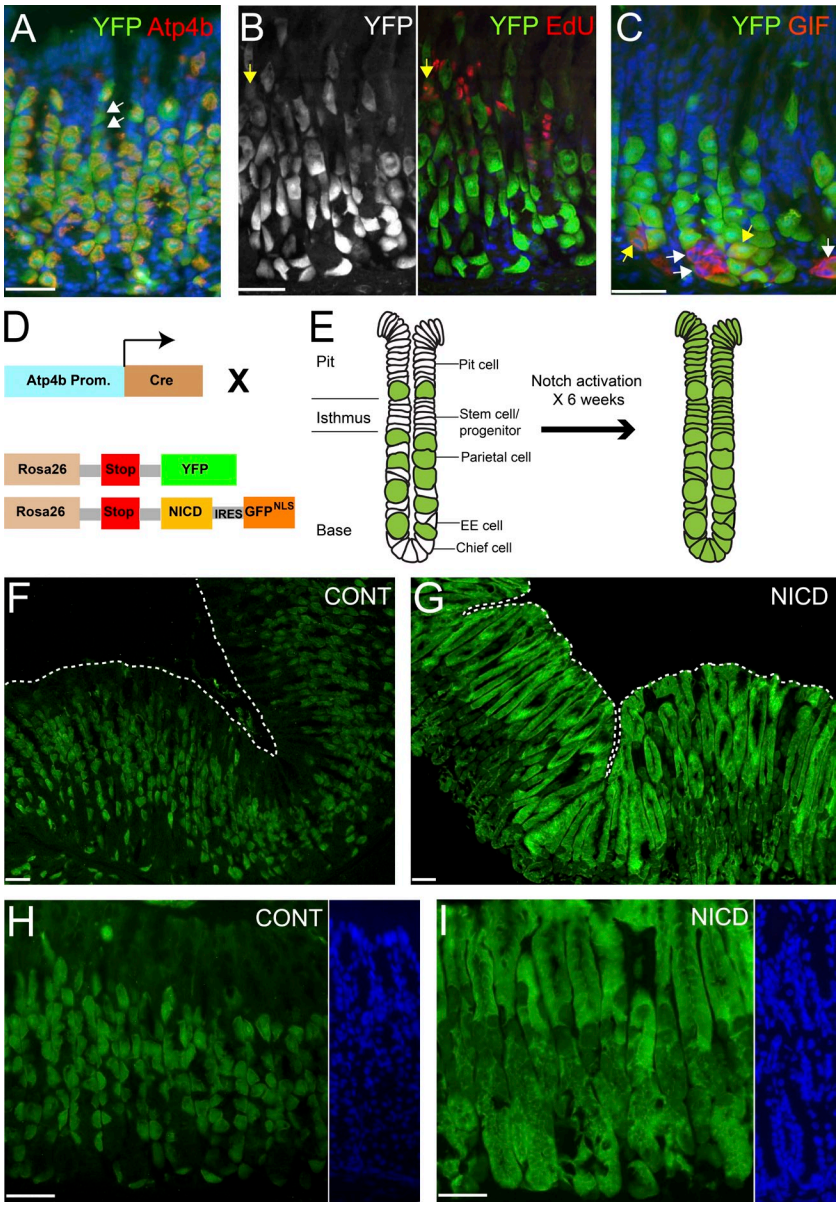

Figure 3. Effects of Notch pathway activation in committed epithelial cells. (A) Cre-dependent YFP expression in all parietal (Atp4b$^+$) and few non-parietal (Atp4b$^-$, arrows) cells in Atp4b-Cre;Rosa26$^{+/YFP}$ mice. (B and C) These rare Atp4b$^-$YFP$^+$ cells represent both a proliferating population (B, EdU$^+$, yellow arrows) and chief cells (C, GIF$^+$, yellow arrows; YFP$^-$ chief cells, representing the majority, are marked with white arrows). (D) Mouse crosses used to drive parietal cell–specific expression of NICD1 and to mark daughter cells with YFP. (E) Illustration of the results of Notch pathway activation in parietal cell precursors, showing the origin of whole gland units from YFP$^+$ stem or multipotential progenitor cells. (F–I) YFP expression in *Atp4b-Cre*;*Rosa26*$^{+/YFP}$ (CONT) and *Atp4b-Cre*;*Rosa26*$^{NICD/YFP}$ (NICD) gastric glands. Dashed lines (F and G) and DAPI staining (H and I) delineate the full mucosal height. Bars, 50 µm. Experiments in A–C used 3 mice, with duplicate staining giving similar results, and experiments in F–I were performed using >10 mice.

in wild-type mice (Fig. S3 C). Most importantly, in examining hundreds of *Atp4b-Cre*;*Rosa26*$^{+/YFP}$ gastric glands, we never observed colocalization of YFP with chromogranin A$^+$ EE cells or with the cells lining gastric pits (Fig. S3, D and E) and never detected YFP expression throughout a gastric gland (Fig. 3, F and H; Fig. S3, D and E; and not depicted). Whereas stem cells give rise to all epithelial cell types, committed progenitors have a more limited cell yield, such as foveolar cells only, or parietal and chief cells (Karam and Leblond, 1993). Occasionally, YFP$^+$ cells in the gastric antrum, where parietal cells are infrequent, also expressed Atp4b (Lee and Leblond, 1985). Thus, the *Atp4b* promoter faithfully drives Cre expression in all parietal cells, rare chief cells, and possibly in bipotential progenitors, but not in stem or multipotent cells.

To induce Notch activity in this differentiated compartment, we crossed *Atp4b-Cre* mice with the *Rosa26*^{NICD} knock-in strain; expression of the Notch1 intracellular domain (NICD1) in these mice requires excision of an upstream Lox-STOP-Lox cassette (Murtaugh et al., 2003). To trace lineages, we retained the Cre-dependent *Rosa26*^{YFP} allele (Fig. 3 D), expecting Cre to both activate the Notch pathway and mark all descendant cells with YFP. The resulting constitutive presence of NICD1 profoundly altered the pattern of YFP staining in gastric glands. In *Atp4b-Cre*;*Rosa26*$^{NICD/YFP}$ mice, most gastric corpus units (mean 92 ± 0.88%) expressed YFP throughout the gland (Fig. 3, E, G, and I), indicating derivation of all resident cells from NICD1-expressing parietal cells. Two possibilities may explain this result: (a) parietal cells with Notch activation outcompete other lineages and occupy whole glands, or (b) parietal cells with Notch activation dedifferentiate into multipotential progenitors or stem cells, giving rise to all lineages. To distinguish between these possibilities, we stained tissues for the chief cell–specific marker Gif, the EE cell product chromogranin A, the parietal cell marker Atp4b, and the foveolar cell–specific dye periodic acid Schiff. YFP signals, which are confined to parietal cells in control mice, were now readily evident in all four epithelial cell types (Fig. 4, A–C, and Fig. S3 F), indicating that they derive from YFP$^+$ progenitors. Notch pathway activation in rare parietal cells present in the antrum also triggered conversion into multipotential cells that reconstituted entire glands (Fig. S3 G). Although the NICD1 transgene contains an IRES-GFP cassette, the low level of nuclear GFP was undetectable by fluorescence

microscopy and did not interfere with robust detection of YFP in the transgenic mice. Nevertheless, to exclude possible fluorescence artifacts in *Rosa26*^{YFP} mice, we crossed the *Rosa26*^{LacZ} allele (Soriano, 1999) into the *Atp4b-Cre*;*Rosa26*^{NICD} background and also observed β-galactosidase staining throughout gland units (Fig. S3 H). GFP immunostaining further confirmed that whole glands were derived from NICD1-expressing cells (unpublished data).

Constitutive Notch activity thus converts cells that are committed to the parietal or a mixed parietal-chief cell lineage into stem or multipotential progenitors that give rise to all stomach epithelial cell types. Glands derived from NICD1-expressing progenitors appeared functionally intact, with all cell types present in normal proportions and location, except for a reduced fraction of EE cells, consistent with the known effect of Notch signaling in inhibiting EE cell differentiation in the intestine. As *Atp4b* gene expression normally initiates by E17, NICD1-induced dedifferentiation could in principle reflect cellular reprogramming during development; in this case, stem-like activity should be apparent at or soon after birth. However, 8- and 15-d old stomachs showed a mosaic of YFP$^+$ and YFP$^-$ glands, with a progressive increase in the YFP$^+$ fraction (Fig. 4 D), and it took 3–6 wk for the vast majority of corpus units to become uniformly labeled. These results demonstrate a gradual conversion of glands in postnatal life.

NICD1-induced dedifferentiation could occur either in mature parietal cells or, if the *Atp4b* transgene is activated earlier, in their precursors. Several observations support the latter possibility. First, YFP or LacZ expression in 6–8% of glands remained confined to parietal cells (Fig. 3 G and Fig. S3 H), which indicates that mature NICD1-expressing

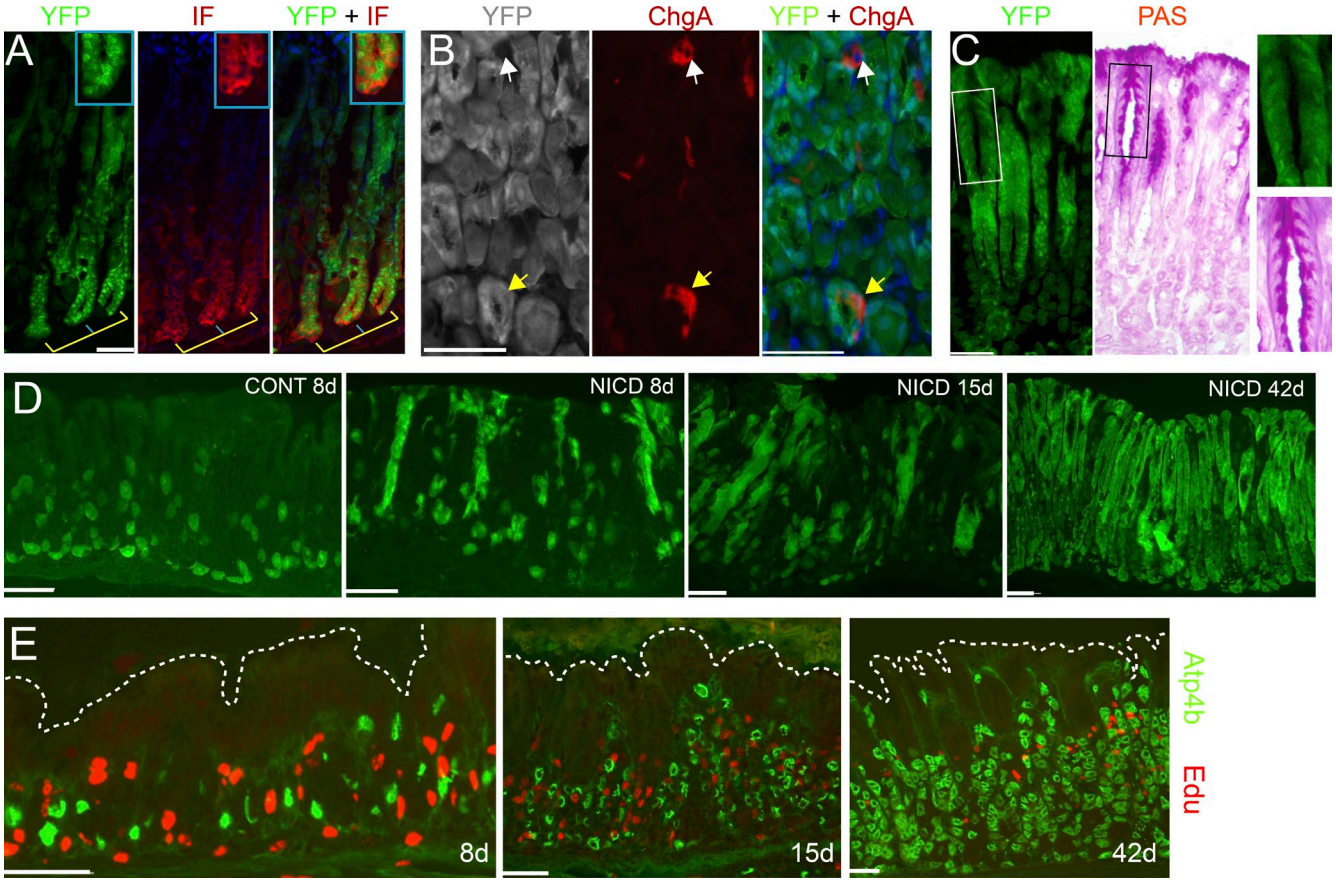

Figure 4. Notch-mediated conversion of parietal cell precursors to multipotential progenitors. (A) Co-localization of YFP with Ab staining for the chief cell–specific marker intrinsic factor (IF). Yellow and blue lines point to the base of three consecutive gastric glands that show IF Ab and YFP signals in the same cells. The gland pointed in blue is shown at high magnification in each inset. (B) Co-localization of YFP with Ab staining for the EE cell–specific marker chromogranin A (ChgA). The yellow arrow points to a typical cell expressing both YFP and ChgA; the white arrow shows ChgA expression in a cell derived from one of the few glands that escape NICD-mediated conversion. (C) Two sequential tissue sections demonstrate broad expression of YFP in foveolar (pit) cells, which stain specifically with periodic acid Schiff (PAS). Boxed areas in the two consecutive images are magnified in the two panels to the far right. (D) Highly mosaic YFP expression in 8- and 15-d-old Atp4b-Cre;Rosa26$^{NICD/YFP}$ stomachs, with total gland involvement by 6 wk. 8-d-old Atp4b-Cre;Rosa26$^{+/YFP}$ CONT stomach is shown in the left image. (E) Nonoverlapping patterns of EdU$^+$ proliferating cells (red) and terminally differentiated Atp4b$^+$ cells (green) in Atp4b-Cre;Rosa26$^{NICD/YFP}$ stomachs. Dashed lines delineate the luminal edge of stomach glands. Bars, 50 µm. All experiments were performed on at least three mice and tissues were stained in duplicate, with similar results.

cells can avoid conversion. Second, rare Gif$^+$ chief cells and EdU-incorporating cells coexpressed YFP (Fig. 3, A–C, arrows), hinting at some Cre-expression within proliferative bipotential precursors. Third, parietal cells greatly outnumber their precursors. Had this number of mature cells converted into progenitors, both gland architecture and cell proportions would be markedly distorted, which was not the case. Indeed, the rate at which whole glands expressed YFP in the first weeks of life (Fig. 4 D) approximates the rate of parietal cell turnover (Karam and Leblond, 1993). Fourth, if mature parietal cells were to dedifferentiate, then it should be possible to capture the progenitor property of cell replication in some cells expressing the terminal marker Atp4b. We therefore analyzed EdU localization in relation to Atp4b expression in mice treated with EdU at different ages. As we observed in wild-type mice (Fig. S3 C), Atp4b and EdU did not localize in the same cells in *Atp4b-Cre*;*Rosa26*$^{NICD/YFP}$ mice (Fig. 4 E). Collectively, these results suggest that a parietal or bipotential precursor is the more likely target of Notch-induced conversion into multipotential progenitors than are fully mature parietal cells.

Notch activity did not seem to interfere with cell maturation or epithelial function, and whole glands remained YFP$^+$ at 18–20 wk, suggesting long-term reconstitution. However, ongoing *Atp4b-Cre* transgene activity precludes making a distinction between continual replenishment of multipotential progenitors and stable conversion into stem cells. As whole glands never expressed YFP in the absence of NICD (Fig. 3, F and H), the important point is that NICD converts a cell that is substantially committed toward lineage differentiation into one that can generate all epithelial cell types.

Notch-induced dedifferentiation leads to formation of adenomas that show focal Wnt pathway activation

Hes1 is overexpressed in intestinal adenomas in *APC*^{Min} mice (van Es et al., 2005), Notch activation increases intestinal adenomas in *APC*$^{+/1638N}$ mice, and Jagged1 haplodeficiency in *APC*^{Min} mice reduces polyp size (Fre et al., 2009; Rodilla et al., 2009). As these observations all point to a role for Notch signaling in intestinal tumorigenesis, we followed the consequences of constitutive Notch activity in the stomach epithelium longitudinally. Between 4 and 8 wk of age, the dramatic effect of NICD1 on stomach cell dedifferentiation was accompanied by overtly normal patterns of cell proliferation (Fig. 5 A). By 18 wk, however, the zone of cell replication in *Atp4b-Cre*;*Rosa26*$^{NICD/YFP}$ stomachs was significantly expanded, well beyond the isthmus (Fig. 5 B), and multiple sessile adenomas became evident. Within these adenomas, proliferation was further increased, replicating cells were distributed haphazardly, and cell nuclei were enlarged and dysplastic (Fig. 5, C–E; Fig. S4; and not depicted). Thus, cells that dedifferentiate as a result of Notch activation proliferate excessively and generate dysplastic adenomas, indicating that Notch activation unmasks a tumorigenic potential latent within parietal cells or their immediate precursors. Incidentally, some foci of dysplasia within adenomas showed loss of the mature cell markers Atp4b and Muc5AC, which were robustly expressed in neighboring tissue but not in these dysplastic foci (Fig. 5, F and G).

Because patients with familial adenomatous polyposis and mice with targeted disruption of the *Apc* tumor suppressor gene develop stomach polyps in addition to intestinal lesions (Offerhaus et al., 1999; Tomita et al., 2007), we examined the gastric adenomas in *Atp4b-Cre*;*Rosa26*^{NICD} mice for evidence of Wnt pathway activation, starting with nuclear localization of the canonical Wnt pathway effector β-catenin (Clevers, 2006). We did not detect nuclear β-catenin in the stomachs of <30-wk-old mice, but focal patches of intense activity appeared in mice by ∼1 yr, comparable to the signal in intestinal adenomas in *Apc*^{Min} mice (Fig. 5 H). In some areas, this signal was confined to the base of stomach corpus glands (Fig. 5 J); in other areas it distributed evenly within adenomas (Fig. 5 H). To verify Wnt pathway activation with other, more sensitive molecular markers, we isolated stomach epithelial cells and used quantitative RT-PCR to measure expression of transcripts that are known to respond to Wnt signaling in antral stomach and intestinal adenomas (Van der Flier et al., 2007; Barker et al., 2010). 5 of the 10 Wnt target genes we assessed in this fashion showed significantly increased levels in *Atp4b-Cre*;*Rosa26*^{NICD} stomach epithelium compared with control littermates (Fig. 5 I). Immunohistochemical examination of two such overexpressed markers, CD44 and Sox9, revealed broader distribution than nuclear β-catenin, but the latter signal always coincided with the other markers (Fig. 5 J). Thus, over time the adenomas that form within NICD-active stomach epithelium show evidence for focal activation of the canonical Wnt signaling pathway.

Adenoma formation upon prolonged Notch activation depends on cellular context

Recently identified stomach stem cells resemble their intestinal counterparts in expressing the surface marker Lgr5, but are restricted to the antral-pyloric segment and a small area of the corpus near the squamo-columnar junction (Fig. 6 A); Wnt activation in Lgr5$^+$ intestinal or stomach antral stem cells induces adenomas (Barker et al., 2009, 2010). To determine if the aberrant cell proliferation induced by Notch activation in dedifferentiated parietal cells would occur in a native stem cell population, we introduced the *Rosa26*^{NICD} and *Rosa26*^{LacZ} alleles into *Lgr5-Cre*$^{(ERT2)}$ mice (Fig. 6 B). Notch-activated Lgr5$^+$ progeny contributed to whole glands in the antrum (Fig. 6 C) and esophageal junction (Fig. 6 D), reflecting known stem cell activity. Expanded cell replication and focal adenomas were always apparent in *Atp4b-Cre*;*Rosa26*^{NICD} mice by 18 wk (Fig. 5 B). In contrast, β-galactosidase–stained gastric glands showed the same, normal pattern of cell proliferation as their neighbors, with no proliferating cells lying outside the isthmus and few if any parietal cells within β-galactosidase$^+$ glands (Fig. 6, C and D). A trivial explanation for the lack of enhanced cell replication could be that Lgr5-Cre is inefficient in excising the Lox-STOP-Lox cassette at the *Rosa26*^{NICD} allele, so that LacZ$^+$ glands may not coexpress NICD. To exclude this possibility, we examined stained tissues for GFP, which is

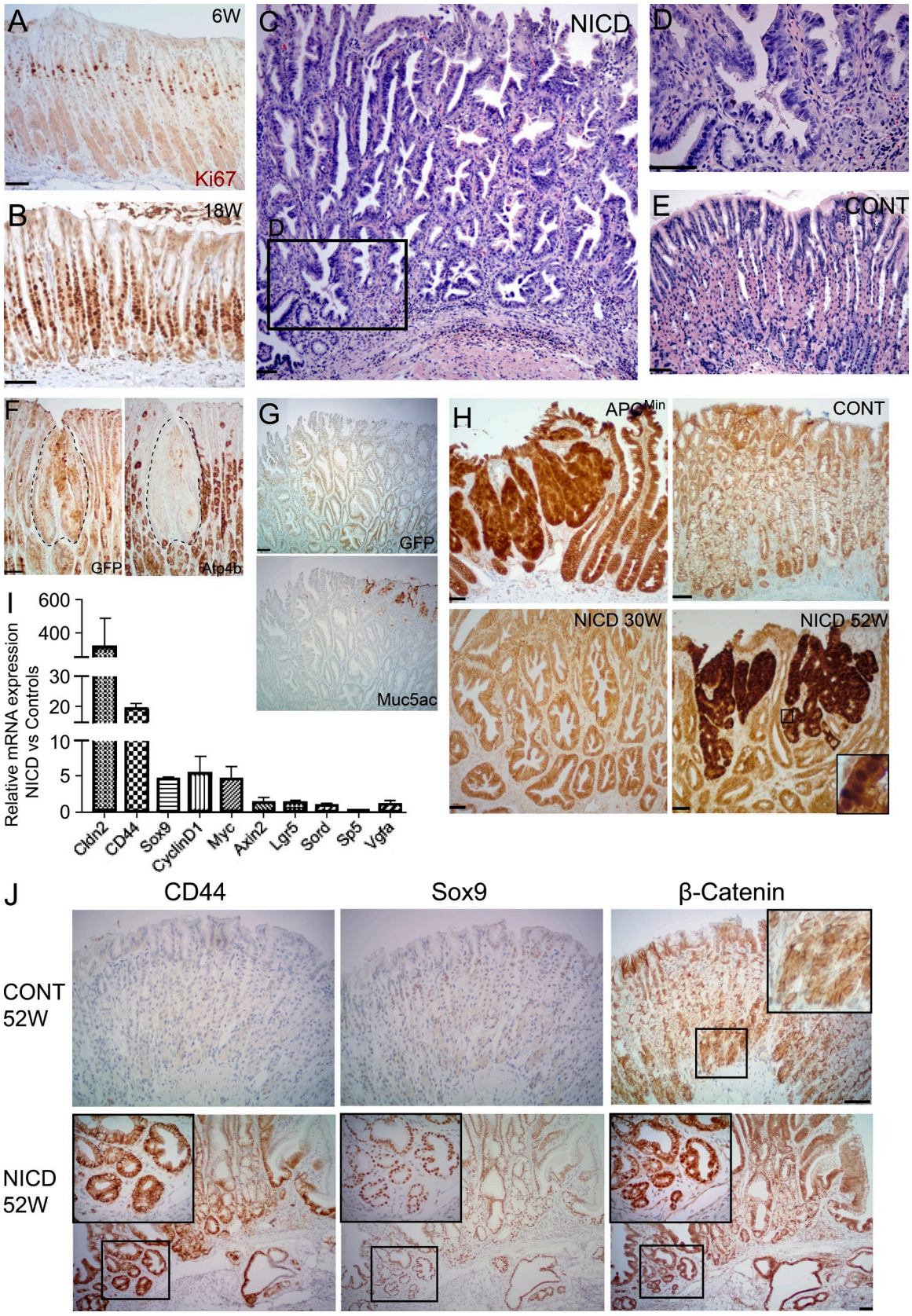

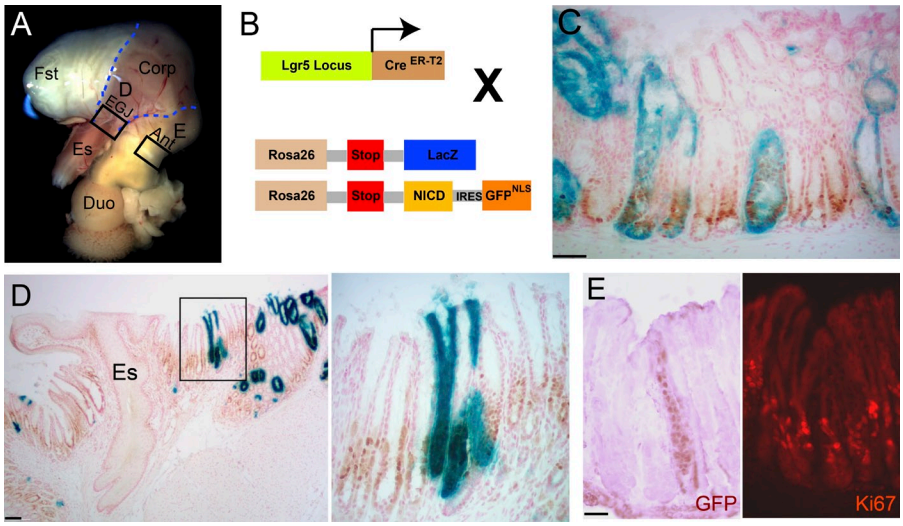

Figure 6. Normal proliferation in response to Notch activation in distal gastric stem cells. (A) Location of gastric regions in adult mouse stomach. Ant, antrum; Corp, corpus; Duo, duodenum; Fst, forestomach; EJ, esophagogastric junction; Es, esophagus. (B) Schema of mouse crosses to generate *Lgr5-Cre*; *Rosa26*$^{NICD/LacZ}$ mice. (C and D) Lgr5^{Cre}-induced Notch activation was traced with β-galactosidase staining (blue color) in gastric antrum (C) and the esophagogastric junction (D). Activation in Lgr5^{+} stem cells does not perturb proliferation (PCNA staining, brown color), even at 18 wk. Bars, 50 µm. The boxed area in D (left) is magnified in the image on the right. (E) Lgr5-Cre–mediated recombination at the Rosa^{NICD} locus was verified by staining for IRES-linked nuclear GFP. GFP^{+} cells show the normal distribution of Ki67^{+} cells at 18 wk. All tissue analyses used four mice and were done in duplicate, with similar results.

expressed as a nucleus-localized protein from an internal ribosome entry site in the NICD construct (Fig. 6 B). Although nuclear GFP was expressed throughout recombined antral glands, the Ki67 proliferation marker was restricted to the typical basal zone of cell replication (Fig. 6 E). Accelerated proliferation and adenomas are thus highly context-dependent in the stomach, occurring uniformly in dedifferentiated corpus stem cells but not in resident Lgr5^{+} antral stem cells.

DISCUSSION

In the digestive epithelium, Notch signaling has been implicated in homeostasis and cell lineage allocation in Wnt-dependent intestinal crypts but its role in the closely related mucosal lining of the stomach is less well understood. Our results reveal Notch signaling both in the developing stomach endoderm and in the isthmus of adult gastric glands, coincident in the latter with an isthmal progenitor population. Blockade of Notch activity impairs epithelial proliferation, whereas constitutive Notch activation in committed parietal cells or bipotential parietal-chief cell precursors has the remarkable effect of gradually converting them into multipotential progenitors. These progenitors initially proliferate normally and give rise to all gastric epithelial cell types. As mice age, gland units derived from NICD1-expressing parietal cells show excessive cell replication and produce adenomas with areas of poor differentiation and foci of Wnt signaling pathway activation. Because Notch activation in resident Lgr5^{+} gastric antral stem cells, in contrast, does not disturb proliferation or produce adenomas, we conclude that dedifferentiation of a committed cell provides a distinctive milieu that is especially sensitive to unregulated Notch signaling.

Signaling mechanisms that regulate stomach epithelial renewal play an important part in the response to injury and in gastric cancer, but are largely unknown. Using pharmacologic inhibition, we demonstrate that, like their intestinal counterparts, gastric stem and progenitor cells also depend on Notch signaling. A slower effect on stomach cell proliferation compared with the intestine might reflect different turnover rates or distinct downstream mechanisms in the two organs. Intestinal cell cycle arrest and secretory cell metaplasia are believed to reflect activation of the transcription factor Math1 (Kazanjian et al., 2010; van Es et al., 2010; Kim and Shivdasani, 2011), which is absent from the stomach (Yang et al., 2001). Thus, stomach Notch signaling probably operates through an alternative factor, which affects cell proliferation less quickly and secretory cells less profoundly than Math1 does in the intestine.

Figure 5. Adenoma formation with focal Wnt pathway activation in progenitors dedifferentiated as a result of unregulated Notch activity. (A and B) The zone of Ki67 staining in *Atp4b-Cre*;*Rosa26*$^{NICD/YFP}$ stomach epithelium at 6 wk (A) and 18 wk (B). (C–E) Hematoxylin and eosin (H&E) staining reveals focal adenomas in 18-wk-old *Atp4b-Cre*;*Rosa26*$^{NICD/YFP}$ stomach (C and D), including subregions of dysplasia with enlarged nuclei and stratified cells. The boxed area in C is shown at higher magnification in D. (E) Gland structure in littermate controls. (F and G) Impaired cell maturation in scattered foci within Notch-induced adenomas. Nuclear GFP stain, a surrogate for NICD expression, is apparent in most cells. The parietal and pit cell markers Atp4b (F) and Muc5AC (G) appear in the expected distribution in much of the tissue, but are absent from some dysplastic areas, such as the dashed area in F and top left of the section in G. (H) Nuclear β-catenin staining, indicating activation of the canonical Wnt signaling pathway, in 52-wk-old mutant mouse stomachs (bottom right; inset shows nuclear localization at high magnification). Also shown are intestinal adenomas in APC^{Min} mice (top left), control littermates (CONT, top right), and younger NICD mutants, e.g., 30 wk (bottom left). (I) Quantitative RT-PCR analysis of Wnt target genes on 1-yr-old *Atp4b-Cre*;*Rosa26*^{NICD} and littermate control stomach epithelial cells. Results are normalized with respect to *Gapdh* mRNA and expressed as the mean ± SD. Total epithelial cells isolated from three mice per genotype were analyzed in duplicate, with similar results. (J) Immunohistochemistry for CD44, Sox9, and β-catenin in control and NICD-expressing mouse stomach. Boxed areas are magnified in the insets. Bars, 50 µm. All tissue analyses used groups of five mice and were done in duplicate, with similar results.

Our most unexpected and unusual finding is that a single in vivo manipulation of parietal cells reprograms cells with restricted potential into those that can produce all stomach epithelial cell lineages. In contrast, lone Notch activation in the intestine alters crypt proliferation subtly and requires a functional Wnt pathway (Fre et al., 2009). This difference might reflect the fact that we activated Notch in committed gastric cells, whereas others used *Villin-Cre* transgenic mice to activate Notch throughout the intestinal epithelium, including native stem cells (Fre et al., 2009). Our results suggest that parietal cell precursors are the likely targets of unregulated Notch activity, but continuous expression of the *Atp4b-Cre* transgene precludes establishing whether they dedifferentiated into bona fide stem cells or multipotent progenitors. Tetracycline control of Cre recombinase activity (Gossen and Bujard, 1992) might, in the future, allow testing of long-term reconstitution to distinguish between these possibilities. A second key question pertains to the mechanisms that act downstream of Notch signaling to induce dedifferentiation. Canonical Wnt signaling controls homeostasis in intestinal crypts and perhaps also in the gastric antrum but not in most of the gastric corpus (Barker et al., 2010). As Wnt signaling is activated only very late and focally after corpus epithelial dedifferentiation, it is not likely to mediate the Notch effect. Four or fewer defined transcription factors can reprogram mature embryonic and adult cells into pluripotent stem cells (Takahashi and Yamanaka, 2006), and it will be interesting to determine if the same factors control the form of reprogramming we report in the stomach in vivo.

Overexpression of Notch receptors 1 and 3 is statistically significant in both the intestinal and diffuse subtypes of human gastric cancer (Chen et al., 2003), hinting at a role for Notch activity in some cases. Furthermore, dedifferentiated progenitors in aged *Atp4b-Cre*;*Rosa26*^{NICD} mice proliferate excessively and eventually develop adenomas, perhaps much as induced pluripotent stem cells are prone to form tumors in mice (Okita et al., 2007). Adenomas in the abnormal gastric epithelium showed small areas of intense nuclear β-catenin signal and increased expression of several Wnt target genes. Among these genes, CD44 was recently proposed as a marker of gastric cancer stem cells (Takaishi et al., 2009). Thus, Notch-mediated dedifferentiation might, over time, increase the pool of potential tumor-initiating cells. Wnt signaling may play a part in human and murine tumors of the gastric antrum (Offerhaus et al., 1999; Tomita et al., 2007), but probably has little role in corpus cancers; the significance of focal Wnt pathway activity in Notch-induced gastric adenomas is uncertain. In our study, Notch activation in gastric antral stem cells did not affect cell proliferation or produce adenomas. Because dedifferentiated progenitors in NICD-expressing gastric epithelium generate all resident cell types and the cell of adenoma origin is therefore unclear, our results suggest the importance of antecedent dedifferentiation in tumor formation. Collectively, our observations reveal a requirement for Notch signaling in gastric epithelial homeostasis, affecting the proper balance between self-renewal and differentiation that is essential to avoid tumors.

MATERIALS AND METHODS

Experimental animals. *RBP-Jκ*$^{Fl/Fl}$ mice (Han et al., 2002) were provided by S. Artavanis-Tsakonas (Harvard Medical School, Boston, MA) with permission from T. Honjo (Kyoto University, Kyoto, Japan). *Osr1-cre* mice (Grieshammer et al., 2008) were provided by G. Martin (University of California, San Francisco, CA). *Atp4b-Cre* mice (Syder et al., 2004) were provided by J. Gordon (Washington University, St. Louis, MO). *Rosa26*^{YFP} (Srinivas et al., 2001), *Rosa26*^{LacZ} (Soriano, 1999), *Rosa26*$^{NICD1\text{-}Ires\text{-}GFP}$ (Murtaugh et al., 2003), and *Lgr5*$^{EGFP\text{-}IRES\text{-}Cre}$ (Barker et al., 2007) mice were purchased from The Jackson Laboratory. *Lgr5-Cre*$^{(ERT2)}$;*Rosa26*^{NICD} and littermate control mice were treated with 2 mg tamoxifen (Invitrogen) by i.p. injection for 5 consecutive days. Animals were housed under specific pathogen–free conditions and handled in accordance with protocols approved and monitored by the Dana-Farber Cancer Institute Animal Care and Use Committee.

DBZ. The γ-secretase inhibitor DBZ was synthesized at Syncom (Groningen), suspended in 0.5% (wt/vol) hydroxypropylmethylcellulose (METHOCEL E4M; Dow Chemicals) and 0.1% (wt/vol) Tween-80 in water, and injected i.p. (20 μmol/kg) on 5 consecutive days.

In situ hybridization. Tissues were fixed overnight in 4% paraformaldehyde at 4°C, embedded in OCT compound (Sakura), cut in 9-μm sections, rehydrated, and treated with 10 μg/ml proteinase K (Roche) followed by 0.1 M triethanolamine in 0.2% acetic anhydride. Samples were hybridized overnight with digoxigenin-labeled antisense probes at 60°C. DNA templates for riboprobes were gifts from A. McMahon (Harvard University, Boston, MA). Slides were washed in 2X SSC, incubated with alkaline phosphatase-conjugated digoxigenin Ab (1:2,000), and treated with nitroblue tetrazolium/5-bromo-4-chloro-3-indolyl phosphate (Roche).

Immunohistochemistry and histology. Tissues were fixed overnight in 4% paraformaldehyde at 4°C, dehydrated, embedded in paraffin, and cut into 5-μm sections. Antigens were retrieved in 10 mM Na citrate buffer (pH 6.0) and endogenous peroxidase activity blocked in methanol and 3% H_2O_2. Frozen tissues were embedded in OCT compound and sectioned at 9-μm thickness. After blocking with 5% fetal bovine serum, samples were incubated with the following Ab: Muc5ac (45M1; 1:500; Novocastra), chromogranin A (1:500; Abcam), *Atp4b* (1:1,000; Thermo Fisher Scientific), GIF (1:20,000; gift from D. Alpers, Washington University, St. Louis, MO), Hes1 (1:1,000; gift from N. Brown, University of Cincinnati, OH), Ki67 (MM1, 1:1,000; Vector Laboratories), PCNA (1:300; Neomarkers), CD44 (1:500; eBioscience), β-catenin (1:500; BD), Sox9 (1:300; Millipore), and TFF3 (1: 300; gift from D. Podolsky, University of Texas Southwestern, Dallas, TX). For immunofluorescence, cryosectioned samples were incubated with Texas red–conjugated anti–mouse or anti–rabbit IgG (1:300; Jackson ImmunoResearch Laboratories) and analyzed using a microscope (Eclipse E800; Nikon). Paraffin-embedded samples were incubated with biotin-conjugated anti–mouse or anti–rabbit IgG (1:300; Vector Laboratories), and color reactions were developed with VECTASTAIN avidin-biotin complex ABC kit (Vector Laboratories) and diaminobenzidine substrate (Sigma-Aldrich). Hes1 staining was amplified with Tyramide Signal Amplification kit (PerkinElmer). Samples were examined with a compound microscope (BX41; Olympus). Paraffin-embedded samples were rehydrated, stained in Alcian blue solution (pH 2.5), and counterstained with nuclear fast red. EdU staining was performed using the Click-iT Edu Alexa Fluor 594 Imaging kit (Invitrogen), following the manufacturer's instructions. We used fluorescence microscopy to count 250 endodermal cells (YFP^+ and YFP^-) at E15 and 200 gastric corpus glands and distal intestinal villi in 7- and 42-d-old *Osr1-Cre*;*RBP-Jκ*$^{+Fl/Fl}$;*Rosa26*^{YFP} mice ($n = 3$ for each stage). $Ki67^+$ cells were counted in 100 vertically sectioned gastric glands from 3 mice for each DBZ treatment condition. Means and SDs were calculated using Microsoft Excel.

LacZ staining. Dissected tissues were frozen immediately in OCT, sectioned at 16 μm thickness, and stained with β-galactosidase kit (Active Motif) according to the manufacturer's protocol.

Quantitative PCR analyses of mouse stomach epithelial cells. Adult mouse stomachs were washed with PBS and incubated in PBS containing 1mM EDTA at 37°C for 30 min. Epithelial cells were collected and their RNA was harvested using TRIzol reagent (Invitrogen) and reverse transcribed using SuperScript enzyme. cDNA was tested by SYBR green master mix (Applied Biosystems) and qPCR using gene-specific primers (Van der Flier et al., 2007; Barker et al., 2010; Spandidos et al., 2010), as follows: Lgr5, forward, 5′-CCTACTCGAAGACTTACCCAGT-3′ and reverse 5′-GCATTGGGGTGAATGATAGCA-3′; SP5, forward, 5′-TGGGTTCACCCTCCAGACTTT-3′ and reverse 5′-CCGGCGAGAACTCGTAAGG-3′; Sord, forward, 5′-GCTAAGGGCGAGAACCTGTC-3′ and reverse 5′-CATGCTCCCAGTAGTGAACATC-3′; CD44, forward, 5′-CACCATTGCCTCAACTGTGC-3′ and reverse 5′-TTGTGGGCTCCTGAGTCTGA-3′; Sox9, forward, 5′-GAGCCGGATCTGAAGAGGGA-3′ and reverse 5′-GCTTGACGTGTGGCTTGTTC-3′; Vegfa, forward, 5′-CTGCCGTCCGATTGAGACC-3′ and reverse 5′-CCCCTCCTTGTACCACTGTC-3′; Cldn2, forward, 5′-GATCGCCACTCCAGCTACTTC-3′ and reverse 5′-CCCTTGGAAAAGCCAACCG-3′; Axin2, forward, 5′-TGACTCTCCTTCCAGATCCCA-3′ and reverse 5′-TGCCCACACTAGGCTGACA-3′; cMyc, forward, 5′-ATGCCCCTCAACGTGAACTTC-3′ and reverse 5′-CGCAACATAGGATGGAGAGCA-3′; cyclinD1, forward, 5′-GCGTACCCTGACACCAATCTC-3′ and reverse 5′-CTCCTCTTCGCACTTCTGCTC-3′. Means and SDs were calculated using Microsoft Excel.

Online supplemental material. Fig. S1 shows broad expression of Notch signaling components in E14 mouse embryos. Fig. S2 demonstrates efficient inhibition of Notch signaling by the inhibitor DBZ in both stomach and intestine, and describes its mild effect on stomach EE cells. Fig. S3 characterizes Atp4b-Cre and describes dedifferentiation by Notch activation in detail. Fig. S4 shows sessile adenoma formation in Notch-activated mouse stomach epithelium at 18 wk. Online supplemental material is available at http://www.jem.org/cgi/content/full/jem.20101737/DC1.

We thank S. Artavanis-Tsakonas for discussions; T. Honjo, S. Artavanis-Tsakonas, G. Martin, U. Grieshammer, and J. Gordon for sharing mouse lines; to D. Alpers, N. Brown, and D. Podolsky for gifts of antibodies; and to D. Breault, E. Espinoza, D. Horst, B. Kim, S. Krasinski, M. Verzi, and J. Woo for critical comments and discussion.

Supported by the Caring for Carcinoid Foundation, grant R01DK081113 from the National Institutes of Health, and the Dana-Farber/Harvard Cancer Center SPORE Program in GI Cancers (P50CA127003).

The authors declare no competing financial interests.

Submitted: 19 August 2010
Accepted: 22 February 2011

REFERENCES

Barker, N., J.H. van Es, J. Kuipers, P. Kujala, M. van den Born, M. Cozijnsen, A. Haegebarth, J. Korving, H. Begthel, P.J. Peters, and H. Clevers. 2007. Identification of stem cells in small intestine and colon by marker gene Lgr5. *Nature*. 449:1003–1007. doi:10.1038/nature06196

Barker, N., R.A. Ridgway, J.H. van Es, M. van de Wetering, H. Begthel, M. van den Born, E. Danenberg, A.R. Clarke, O.J. Sansom, and H. Clevers. 2009. Crypt stem cells as the cells-of-origin of intestinal cancer. *Nature*. 457:608–611. doi:10.1038/nature07602

Barker, N., M. Huch, P. Kujala, M. van de Wetering, H.J. Snippert, J.H. van Es, T. Sato, D.E. Stange, H. Begthel, M. van den Born, et al. 2010. Lgr5(+ve) stem cells drive self-renewal in the stomach and build long-lived gastric units in vitro. *Cell Stem Cell*. 6:25–36. doi:10.1016/j.stem.2009.11.013

Chen, X., S.Y. Leung, S.T. Yuen, K.M. Chu, J. Ji, R. Li, A.S. Chan, S. Law, O.G. Troyanskaya, J. Wong, et al. 2003. Variation in gene expression patterns in human gastric cancers. *Mol. Biol. Cell*. 14:3208–3215. doi:10.1091/mbc.E02-12-0833

Clevers, H. 2006. Wnt/beta-catenin signaling in development and disease. *Cell*. 127:469–480. doi:10.1016/j.cell.2006.10.018

Fre, S., M. Huyghe, P. Mourikis, S. Robine, D. Louvard, and S. Artavanis-Tsakonas. 2005. Notch signals control the fate of immature progenitor cells in the intestine. *Nature*. 435:964–968. doi:10.1038/nature03589

Fre, S., S.K. Pallavi, M. Huyghe, M. Laé, K.P. Janssen, S. Robine, S. Artavanis-Tsakonas, and D. Louvard. 2009. Notch and Wnt signals cooperatively control cell proliferation and tumorigenesis in the intestine. *Proc. Natl. Acad. Sci. USA*. 106:6309–6314. doi:10.1073/pnas.0900427106

Gossen, M., and H. Bujard. 1992. Tight control of gene expression in mammalian cells by tetracycline-responsive promoters. *Proc. Natl. Acad. Sci. USA*. 89:5547–5551. doi:10.1073/pnas.89.12.5547

Grieshammer, U., P. Agarwal, and G.R. Martin. 2008. A Cre transgene active in developing endodermal organs, heart, limb, and extra-ocular muscle. *Genesis*. 46:69–73. doi:10.1002/dvg.20366

Han, H., K. Tanigaki, N. Yamamoto, K. Kuroda, M. Yoshimoto, T. Nakahata, K. Ikuta, and T. Honjo. 2002. Inducible gene knockout of transcription factor recombination signal binding protein-J reveals its essential role in T versus B lineage decision. *Int. Immunol*. 14:637–645. doi:10.1093/intimm/dxf030

Hattori, T., and S. Fujita. 1976. Tritiated thymidine autoradiographic study of cell migration and renewal in the pyloric mucosa of golden hamsters. *Cell Tissue Res*. 175:49–57. doi:10.1007/BF00220822

Iso, T., L. Kedes, and Y. Hamamori. 2003. HES and HERP families: multiple effectors of the Notch signaling pathway. *J. Cell. Physiol*. 194:237–255. doi:10.1002/jcp.10208

Jensen, J., E.E. Pedersen, P. Galante, J. Hald, R.S. Heller, M. Ishibashi, R. Kageyama, F. Guillemot, P. Serup, and O.D. Madsen. 2000. Control of endodermal endocrine development by Hes-1. *Nat. Genet*. 24:36–44. doi:10.1038/71657

Karam, S.M., and C.P. Leblond. 1993. Dynamics of epithelial cells in the corpus of the mouse stomach. I. Identification of proliferative cell types and pinpointing of the stem cell. *Anat. Rec*. 236:259–279. doi:10.1002/ar.1092360202

Kazanjian, A., T. Noah, D. Brown, J. Burkart, and N.F. Shroyer. 2010. Atonal homolog 1 is required for growth and differentiation effects of notch/gamma-secretase inhibitors on normal and cancerous intestinal epithelial cells. *Gastroenterology*. 139:918–928: 928: e1–e6. doi:10.1053/j.gastro.2010.05.081

Kim, T.H., and R.A. Shivdasani. 2011. Genetic evidence that intestinal notch functions vary regionally and operate through a common mechanism of math1 repression. *J. Biol. Chem*. doi:10.1074.jbc.M110.188797

Kopan, R., and M.X. Ilagan. 2009. The canonical Notch signaling pathway: unfolding the activation mechanism. *Cell*. 137:216–233. doi:10.1016/j.cell.2009.03.045

Laky, K., and B.J. Fowlkes. 2007. Presenilins regulate alphabeta T cell development by modulating TCR signaling. *J. Exp. Med*. 204:2115–2129. doi:10.1084/jem.20070550

Lee, E.R., and C.P. Leblond. 1985. Dynamic histology of the antral epithelium in the mouse stomach: II. Ultrastructure and renewal of isthmal cells. *Am. J. Anat*. 172:205–224. doi:10.1002/aja.1001720304

Lee, E.R., J. Trasler, S. Dwivedi, and C.P. Leblond. 1982. Division of the mouse gastric mucosa into zymogenic and mucous regions on the basis of gland features. *Am. J. Anat*. 164:187–207. doi:10.1002/aja.1001640302

Milano, J., J. McKay, C. Dagenais, L. Foster-Brown, F. Pognan, R. Gadient, R.T. Jacobs, A. Zacco, B. Greenberg, and P.J. Ciaccio. 2004. Modulation of notch processing by gamma-secretase inhibitors causes intestinal goblet cell metaplasia and induction of genes known to specify gut secretory lineage differentiation. *Toxicol. Sci*. 82:341–358. doi:10.1093/toxsci/kfh254

Murtaugh, L.C., B.Z. Stanger, K.M. Kwan, and D.A. Melton. 2003. Notch signaling controls multiple steps of pancreatic differentiation. *Proc. Natl. Acad. Sci. USA*. 100:14920–14925. doi:10.1073/pnas.2436557100

Offerhaus, G.J., M.M. Entius, and F.M. Giardiello. 1999. Upper gastrointestinal polyps in familial adenomatous polyposis. *Hepatogastroenterology*. 46:667–669.

Ohtsuka, T., M. Ishibashi, G. Gradwohl, S. Nakanishi, F. Guillemot, and R. Kageyama. 1999. Hes1 and Hes5 as notch effectors in mammalian neuronal differentiation. *EMBO J*. 18:2196–2207. doi:10.1093/emboj/18.8.2196

Okita, K., T. Ichisaka, and S. Yamanaka. 2007. Generation of germline-competent induced pluripotent stem cells. *Nature*. 448:313–317. doi:10.1038/nature05934

Riccio, O., M.E. van Gijn, A.C. Bezdek, L. Pellegrinet, J.H. van Es, U. Zimber-Strobl, L.J. Strobl, T. Honjo, H. Clevers, and F. Radtke. 2008. Loss of intestinal crypt progenitor cells owing to inactivation of both Notch1 and Notch2 is accompanied by derepression of CDK inhibitors p27Kip1 and p57Kip2. *EMBO Rep.* 9:377–383. doi:10.1038/embor.2008.7

Rodilla, V., A. Villanueva, A. Obrador-Hevia, A. Robert-Moreno, V. Fernández-Majada, A. Grilli, N. López-Bigas, N. Bellora, M.M. Albà, F. Torres, et al. 2009. Jagged1 is the pathological link between Wnt and Notch pathways in colorectal cancer. *Proc. Natl. Acad. Sci. USA.* 106:6315–6320. doi:10.1073/pnas.0813221106

Schröder, N., and A. Gossler. 2002. Expression of Notch pathway components in fetal and adult mouse small intestine. *Gene Expr. Patterns.* 2:247–250. doi:10.1016/S1567-133X(02)00060-1

Soriano, P. 1999. Generalized lacZ expression with the ROSA26 Cre reporter strain. *Nat. Genet.* 21:70–71. doi:10.1038/5007

Spandidos, A., X. Wang, H. Wang, and B. Seed. 2010. PrimerBank: a resource of human and mouse PCR primer pairs for gene expression detection and quantification. *Nucleic Acids Res.* 38:D792–D799. doi:10.1093/nar/gkp1005

Srinivas, S., T. Watanabe, C.S. Lin, C.M. William, Y. Tanabe, T.M. Jessell, and F. Costantini. 2001. Cre reporter strains produced by targeted insertion of EYFP and ECFP into the ROSA26 locus. *BMC Dev. Biol.* 1:4. doi:10.1186/1471-213X-1-4

Stanger, B.Z., R. Datar, L.C. Murtaugh, and D.A. Melton. 2005. Direct regulation of intestinal fate by Notch. *Proc. Natl. Acad. Sci. USA.* 102:12443–12448. doi:10.1073/pnas.0505690102

Syder, A.J., S.M. Karam, J.C. Mills, J.E. Ippolito, H.R. Ansari, V. Farook, and J.I. Gordon. 2004. A transgenic mouse model of metastatic carcinoma involving transdifferentiation of a gastric epithelial lineage progenitor to a neuroendocrine phenotype. *Proc. Natl. Acad. Sci. USA.* 101:4471–4476. doi:10.1073/pnas.0307983101

Takahashi, K., and S. Yamanaka. 2006. Induction of pluripotent stem cells from mouse embryonic and adult fibroblast cultures by defined factors. *Cell.* 126:663–676. doi:10.1016/j.cell.2006.07.024

Takaishi, S., T. Okumura, S. Tu, S.S. Wang, W. Shibata, R. Vigneshwaran, S.A. Gordon, Y. Shimada, and T.C. Wang. 2009. Identification of gastric cancer stem cells using the cell surface marker CD44. *Stem Cells.* 27:1006–1020. doi:10.1002/stem.30

Tomita, H., Y. Yamada, T. Oyama, K. Hata, Y. Hirose, A. Hara, T. Kunisada, Y. Sugiyama, Y. Adachi, H. Linhart, and H. Mori. 2007. Development of gastric tumors in Apc(Min/+) mice by the activation of the beta-catenin/Tcf signaling pathway. *Cancer Res.* 67:4079–4087. doi:10.1158/0008-5472.CAN-06-4025

van der Flier, L.G., and H. Clevers. 2009. Stem cells, self-renewal, and differentiation in the intestinal epithelium. *Annu. Rev. Physiol.* 71:241–260. doi:10.1146/annurev.physiol.010908.163145

Van der Flier, L.G., J. Sabates-Bellver, I. Oving, A. Haegebarth, M. De Palo, M. Anti, M.E. Van Gijn, S. Suijkerbuijk, M. Van de Wetering, G. Marra, and H. Clevers. 2007. The Intestinal Wnt/TCF Signature. *Gastroenterology.* 132:628–632. doi:10.1053/j.gastro.2006.08.039

van Es, J.H., M.E. van Gijn, O. Riccio, M. van den Born, M. Vooijs, H. Begthel, M. Cozijnsen, S. Robine, D.J. Winton, F. Radtke, and H. Clevers. 2005. Notch/gamma-secretase inhibition turns proliferative cells in intestinal crypts and adenomas into goblet cells. *Nature.* 435:959–963. doi:10.1038/nature03659

van Es, J.H., N. de Geest, M. van de Born, H. Clevers, and B.A. Hassan. 2010. Intestinal stem cells lacking the Math1 tumour suppressor are refractory to Notch inhibitors. *Nat. Commun.* 1:1–5. doi:10.1038/ncomms1017

Yang, Q., N.A. Bermingham, M.J. Finegold, and H.Y. Zoghbi. 2001. Requirement of Math1 for secretory cell lineage commitment in the mouse intestine. *Science.* 294:2155–2158. doi:10.1126/science.1065718

SUPPLEMENTAL MATERIAL

Kim and Shivdasani, http://www.jem.org/cgi/content/full/jem.20101737/DC1

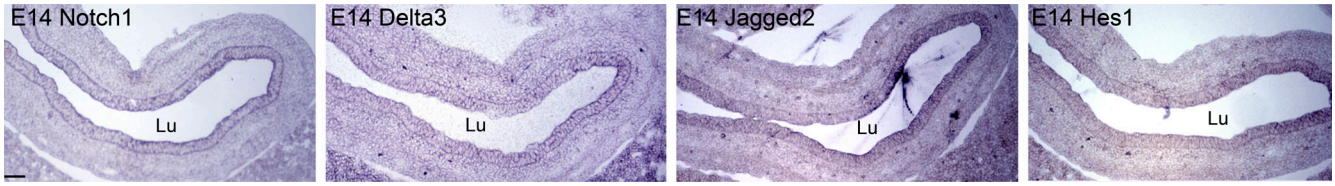

Figure S1. Broad expression of Notch signaling components. In situ hybridization of mouse stomachs at E14 with Notch1, ligands Jagged 2 and Delta3, and Hes1. Lu, gastric lumen. Bar, 50 µm. Experiments were repeated twice, with similar results.

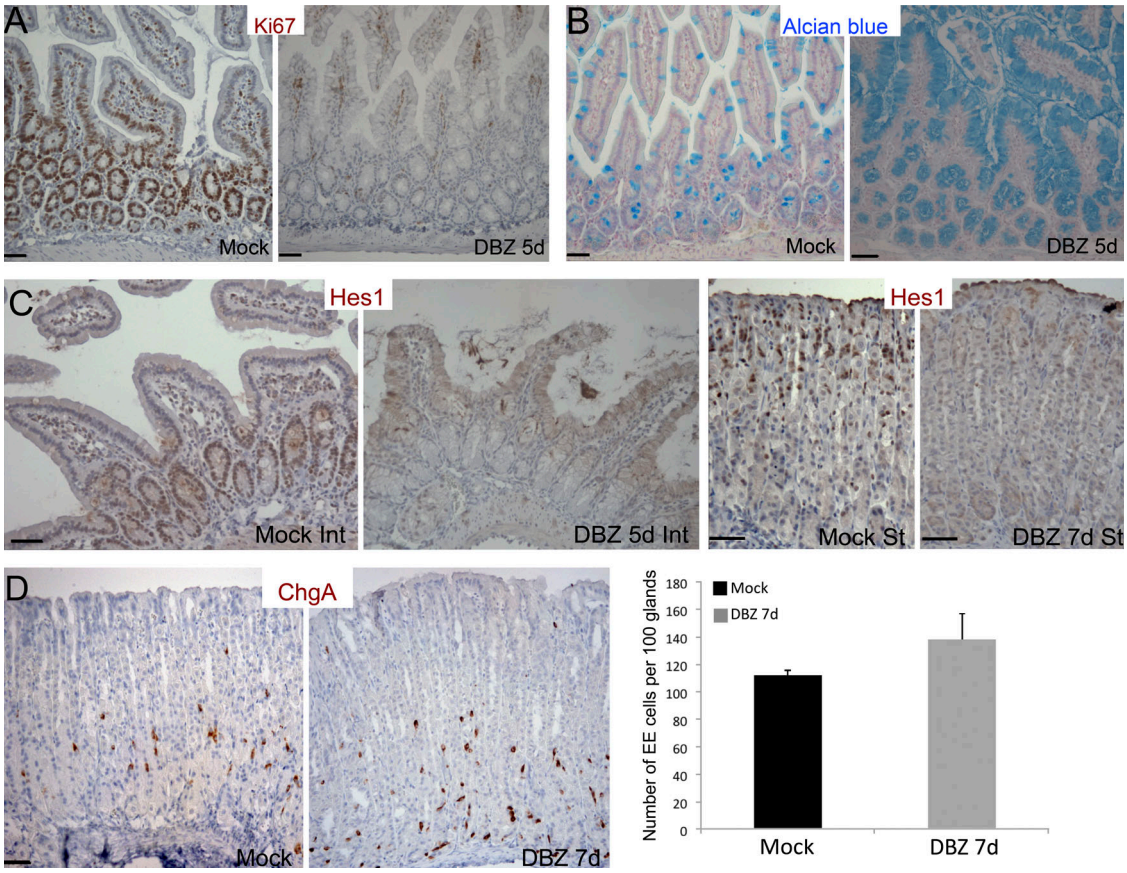

Figure S2. Effects of pharmacologic inhibition of the Notch pathway in adult mouse gut. (A and B) Reproducible replication arrest and goblet cell metaplasia in intestinal epithelium after treatment with 20 µmol/kg DBZ, revealed by staining with Ki67 Ab (A) or Alcian blue dye (B). (C) DBZ abolished Hes1 expression in intestine (Int) and stomach (St). (D) Chromogranin A^+ EE cells were mildly increased in DBZ-treated mice. Bars, 50 µm. Quantification in D was made using three mice per group, and all other experiments were repeated twice, with similar results. Error bars represent standard deviations.

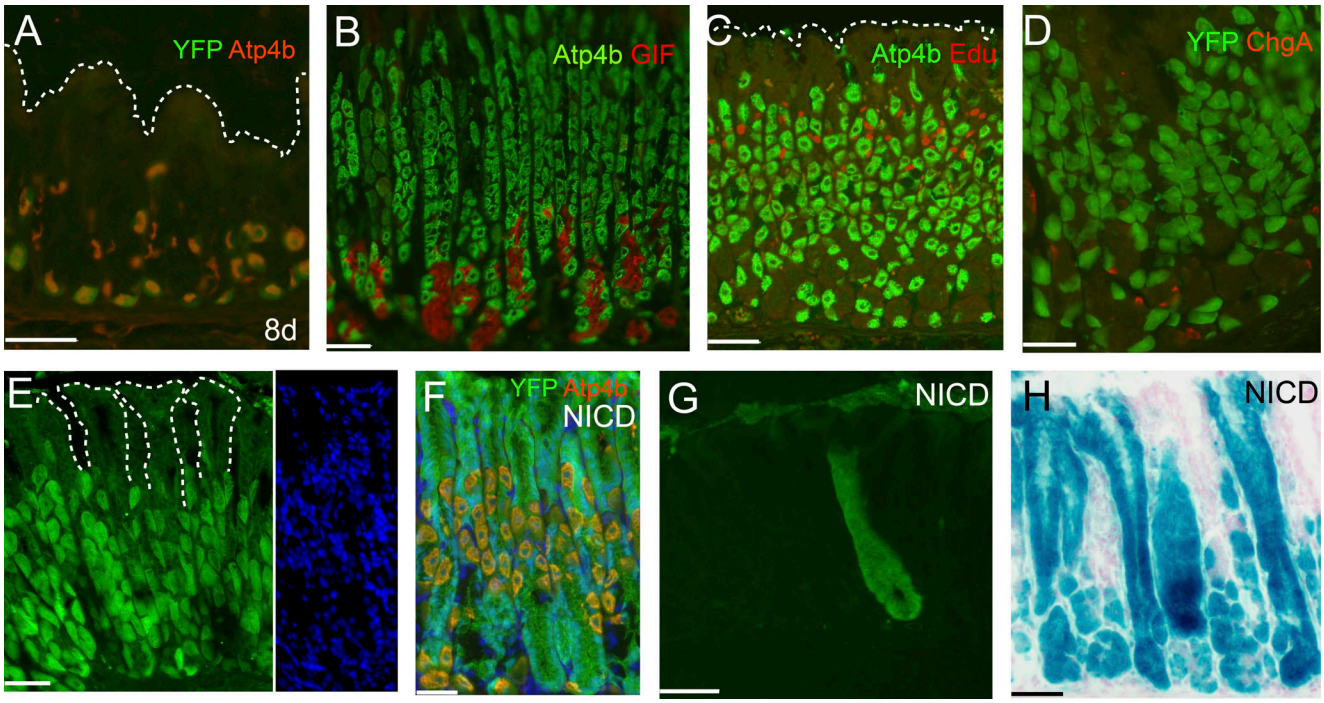

Figure S3. Characterization of Atp4b-Cre and dedifferentiation by Notch activation. (A) Co-labeling of YFP and Atp4b in 8-d-old Atp4b-Cre;Rosa26$^{+/YFP}$ mice. (B) Nonoverlapping expression of chief (GIF) and parietal (Atp4b) cell differentiation markers. (C) Lack of proliferation (EdU uptake) in fully differentiated, Atp4b-expressing parietal cells. (D and E) YFP^{+} cells in Atp4b-Cre;Rosa26$^{+/YFP}$ mouse stomach never express the EE marker chromogranin A (D), nor are they ever present in the pit-cell zone bordering the stomach lumen (E). DAPI nuclear staining of full glands is shown to the right. (F) YFP^{+} cells in 6-wk-old Atp4b-Cre;Rosa26$^{NICD/YFP}$ mouse stomach form mature, Atp4b^{+} parietal cells. (G) Occasionally, glands that were fully YFP^{+} were found in the Atp4b-Cre;Rosa26$^{NICD/YFP}$ stomach antrum. (H) As with the YFP reporter, Atp4b-Cre;Rosa26$^{NICD1/LacZ}$ mice also show fully β-gal^{+} gastric glands, mixed with occasional glands showing persistent parietal cell–restricted β-gal expression. Dashed lines (A, C, and E) demarcate the luminal edge of stomach glands. Bars, 50 µm. All experiments used at least four mice per group, and stains were done in duplicate, with similar results.

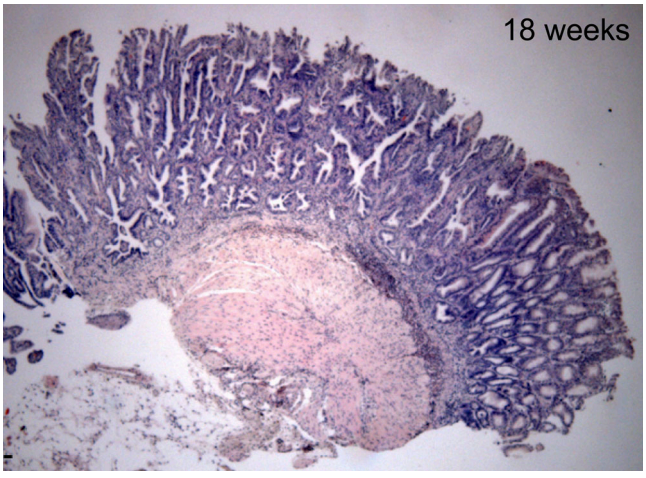

Figure S4. Delayed formation of sessile adenomas upon constitutive Notch activation. Low-magnification view of H&E-stained 18-wk-old Atp4b-Cre;Rosa26$^{NICD/YFP}$ stomach. Bar, 50 µm. Experiments were repeated twice using five mice, with similar results.